

Saturation effects in degenerate four-wave mixing on homogeneously broadened coupled transitions

Govind P. Agrawal

Bell Laboratories, Murray Hill, New Jersey 07974

(Received 4 May 1983)

An analytic nonperturbative treatment of degenerate four-wave mixing is presented to study Zeeman-coherence effects in phase conjugation. The counterpropagating pump waves are taken to be orthogonally circularly polarized and interact with different Zeeman sublevels. The nonlinear medium is modeled in terms of a homogeneously broadened, folded three-level system. Particular attention is paid to the phase-conjugate spectrum obtained by varying the Larmor frequency associated with the Zeeman splitting. A level-crossing resonance is found to occur in the saturation regime and manifests itself as a narrow peak or dip depending on various level decay rates. Even for a purely absorptive system, the Zeeman coupling of the ground-state degenerate sublevels is shown to produce significant phase-conjugate reflectivities at pump intensities much lower than those required for a two-level system.

I. INTRODUCTION

Nonlinear optical phase conjugation^{1,2} is a subject of considerable interest in view of its potential application in adaptive optics, real-time holography, and high-resolution spectroscopy. A powerful technique to generate phase-conjugate wave fronts is resonant degenerate four-wave mixing (DFWM). If the four interacting waves have identical frequencies and polarizations, the two-level model of Abrams and Lind³ provides a nonperturbative analysis of DFWM under one-photon resonance conditions. Since its introduction this model has been extended in several directions.⁴⁻⁶ In particular, the pump-imbalance-induced splitting of DFWM spectra has recently been predicted^{5,6} and observed by Agrawal *et al.*⁵

Under some experimental situations the four interacting waves, although degenerate in frequency, are chosen to have nonidentical polarizations. The use of orthogonally polarized pump and probe beams in the collinear geometry has the advantage of providing increased interaction length. The counterpropagating pump beams with orthogonal circular polarizations are necessary for vectorial phase conjugation⁷⁻⁹ and, furthermore, avoid spatial hole-burning that is known³ to considerably reduce the DFWM efficiency. The use of nonidentically polarized optical beams for resonant DFWM, in general, requires that level degeneracy, related to angular momenta of the atomic or molecular energy states, should be incorporated in the theoretical analysis. Recently, the level-degeneracy effects have been considered¹⁰⁻¹³ with particular attention paid to the generation of Zeeman coherence that provides a distinct new mechanism for phase conjugation. Motivated by the spectroscopic applications, Doppler broadening has been of major concern in the previous work.¹⁰⁻¹³ There, the analysis is developed using third-order perturbation theory and therefore ignores saturation effects.

The purpose of the present paper is to present a nonperturbative treatment of DFWM in a homogeneously

broadened medium whose resonance behavior can be modeled in terms of a three-level system.¹⁴ More specifically, we consider the Λ configuration where the forward and the backward pump waves with orthogonal circular polarizations interact with different one-photon transitions sharing a common upper level (see Fig. 1). The two-photon coupling of these dipole-allowed transitions generates Zeeman coherence¹⁰⁻¹⁵ among the lower-state sublevels and plays an important role in the description of DFWM. Experimentally, the situation can be realized using the $J=1 \rightarrow J=0$ transition of an atomic system. Since Doppler broadening is ignored, the analysis is more directly applicable to the case of an atomic beam.

The DFWM configuration shown in Fig. 1 should be distinguished with the one considered in Ref. 14 where the four waves were assumed to have identical polarizations. In that case the counterpropagating pump waves form a standing wave which interacts with both of the one-

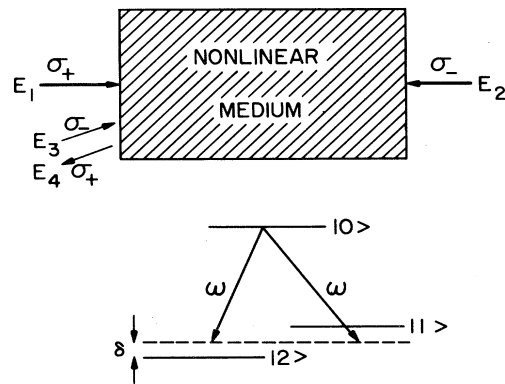


FIG. 1. Illustration of the geometry and the transition scheme used for degenerate four-wave mixing. Here σ_+ and σ_- denote right and left circular polarizations, respectively.

photon transitions. Furthermore, two closely spaced levels of such a three-level system do not correspond to Zeeman sublevels but are usually related to hyperfine components. The use of Zeeman sublevels has an obvious experimental advantage for their spacing can be controlled through a magnetic field.

In order to make the problem analytically tractable the laser frequency is assumed to coincide with the one-photon transition frequency. Dispersive effects are, however, included through the Zeeman splitting of the degenerate lower level. Our analysis shows that the Zeeman coupling of the lower-state sublevels is capable of producing significant phase-conjugate reflectivities at pump intensities much lower than those required for a two-level system (with nondegenerate atomic states). In view of the potential spectroscopic applications, particular attention is paid to the DFWM spectrum obtained by varying the Zeeman splitting (i.e., the Larmor frequency) at a fixed laser frequency. In the saturation regime the line shape exhibits a narrow level-crossing resonance that manifests as a central peak or dip depending on various level-decay rates. The width of this resonance is related to the Zeeman-coherence decay rate and can be much less than the natural width of the one-photon transition.

This paper is organized as follows. The DFWM configuration with orthogonally polarized pump beams is discussed in Sec. II where an expression for the phase-conjugate reflectivity is obtained in terms of the intensity-dependent susceptibility and its derivatives. An analytic expression for this susceptibility is obtained in Sec. III that also states various assumptions and approximations involved in modeling the response of the nonlinear medium. Mathematical details of the susceptibility derivation can be found in the Appendix. Section III also discusses various physical mechanisms that give rise to DFWM. The reflectivity behavior as a function of various parameters such as the pump intensities, the Zeeman splitting, and the relaxation rates is considered in Sec. IV with particular attention paid to the level-crossing DFWM spectrum. Section V is concerned with vectorial phase conjugation and polarization anisotropy in the DFWM response. Finally, the results are discussed in Sec. VI together with the limitations, the possible generalizations and the applications of the theoretical analysis presented here.

II. PHASE-CONJUGATE REFLECTIVITY

In the DFWM geometry shown in Fig. 1 the nonlinear medium is pumped using two orthogonally circularly polarized pump beams E_1 and E_2 which counterpropagate along the z axis. For the sake of definiteness, the forward and the backward pump waves are assumed to have σ_+ and σ_- polarizations, respectively. The probe wave E_3 , propagating along the z' axis at the same optical frequency ω , generates the conjugate wave E_4 through DFWM with polarizations orthogonal to that of E_3 . The probe polarization can be chosen to be σ_+ or σ_- . We consider the case of σ_- polarization since a collinear geometry can be used in that case. The analysis is, however, equally applicable to the case of σ_+ probe-polarization with minor

modifications described later.

The four-wave interaction inside the nonlinear medium is described using the wave equation

$$\nabla^2 \vec{E} - \frac{1}{c^2} \frac{\partial^2 \vec{E}}{\partial t^2} = \mu_0 \frac{\partial^2 \vec{P}}{\partial t^2}, \quad (1)$$

where c is the vacuum velocity of light, μ_0 is the vacuum permeability, and the total electric field

$$\vec{E} = \frac{1}{2} (E'_1 \hat{e}_R + E'_2 \hat{e}_L) e^{-i\omega t} + \text{c.c.} \quad (2)$$

consists of the right (σ_+) and left (σ_-) circularly polarized waves, \hat{e}_R and \hat{e}_L being the corresponding complex unit vectors. In the geometry of Fig. 1 the fields E'_1 and E'_2 are given by

$$E'_1 = E_1 + E_4 = A_1 e^{ikz} + A_4 e^{-ikz'}, \quad (3a)$$

$$E'_2 = E_2 + E_3 = A_2 e^{-ikz} + A_3 e^{ikz'}, \quad (3b)$$

where A_n is the slowly varying amplitude of the field E_n .

In the continuous-wave (cw) case considered here,¹⁶ the induced polarization $\vec{P}(\vec{r}, t)$ can be expressed in terms of the steady-state susceptibilities as follows:

$$\vec{P} = \frac{1}{2} \epsilon_0 (\chi_1 E'_1 \hat{e}_R + \chi_2 E'_2 \hat{e}_L) e^{-i\omega t} + \text{c.c.}, \quad (4)$$

where ϵ_0 is the vacuum permittivity and χ_1 and χ_2 are the medium susceptibilities for the right and left circularly polarized waves. The exact form of χ_n depends on the details of atomic interaction and will be considered in Sec. III. For the time being we leave it unspecified except for noting that the field dependence of $\chi_n(E'_1, E'_2)$ is responsible for DFWM. On substituting Eqs. (2) and (4) in Eq. (1), we obtain the coupled set

$$(\nabla^2 + k^2) E'_n = -k^2 \chi_n(E'_1, E'_2) E'_n, \quad (5)$$

where $k = \omega/c$ and $n=1$ and $n=2$ for σ_+ and σ_- polarizations, respectively.

The phase-conjugate reflectivity R is obtained following a procedure similar to that of Abrams and Lind³ and generalized to account for the orthogonally polarized pump beams.¹⁷ Assuming $|E_4| \ll |E_1|$ and $|E_3| \ll |E_2|$, the susceptibility $\chi_n(E'_1, E'_2)$ is expanded around E_1 and E_2 and only the terms linear in E_3 and E_4 are retained. Using Eqs. (3) and (5) and making the plane-wave approximation, we obtain

$$\frac{dA_n}{dz} = \pm \frac{ik}{2} \chi_n(A_1, A_2) A_n, \quad n=1,2 \quad (6)$$

$$\frac{dA_3}{dz'} = -\alpha_3 A_3 + i\kappa_{34} A_4^*, \quad (7)$$

$$\frac{dA_4^*}{dz'} = \alpha_4^* A_4^* + i\kappa_{43}^* A_3, \quad (8)$$

where the saturated-absorption and the nonlinear-coupling coefficients are given by

$$\alpha_{5-n} = (-ik/2)(\chi_n + |A_n|^2 \chi_{nn}), \quad (9a)$$

$$\kappa_{34} = (k/2) A_1 A_2 \chi_{21}, \quad (9b)$$

$$\kappa_{43} = (k/2) A_1 A_2 \chi_{12}, \quad (9c)$$

and $\chi_{mn} = (\partial\chi_m/\partial|A_n|^2)$ is the susceptibility derivative. Pump depletion has been neglected but Eq. (6) takes into account pump absorption. Considerable simplification occurs if pump absorption is also ignored. The coefficients α_n and κ_{mn} are then independent of z' and Eqs. (7) and (8) can readily be solved. Using the boundary condition that $A_4^*(L) = 0$, where L is the length of the nonlinear medium along the z' axis, the phase-conjugate reflectivity is given by³

$$R = \left| \frac{A_4^*(0)}{A_3(0)} \right|^2 = \left| \frac{\kappa_{43}}{\alpha + g \cot(gL)} \right|^2, \quad (10)$$

where

$$\alpha = (\alpha_3 + \alpha_4^*)/2, \quad (11a)$$

$$g = (\kappa_{43}\kappa_{34} - \alpha^2)^{1/2}. \quad (11b)$$

Equations (9)–(11) complete our description of DFWM for orthogonally polarized pump beams. Once the nonlinear susceptibilities χ_1 and χ_2 are known, the coefficients α_n and κ_{mn} can be evaluated using Eq. (9) and their use in Eq. (10) yields the phase-conjugate reflectivity as a function of various system parameters.

III. NONLINEAR SUSCEPTIBILITY

The nonlinear susceptibility χ_n depends on the details of matter-radiation interaction. We assume that the laser frequency ω is close to the transition frequency ω_a between two atomic (or molecular) energy states and the radiation coupling to other atomic states can be neglected. Each atomic state is $(2J+1)$ -fold degenerate owing to its angular momentum J . For arbitrary J values the density-matrix formalism generally requires an irreducible-tensor representation of the density operator.^{18,19} However, for the specific case of $J=1 \rightarrow J=0$ transition shown in Fig. 1 the resonance behavior can be modeled in terms of a Λ -type three-level system.^{20–25} In the absence of a magnetic field the two lower levels are degenerate and correspond to $m = \pm 1$ Zeeman sublevels of the ground state.

In order to incorporate the saturation effects, we require the steady-state solution of the density-matrix equations obtained for a three-level system interacting with two *arbitrarily strong* optical fields.^{21–24} These equations and the details of their solution are presented in the Appendix. Although a nonperturbative steady-state solution can be obtained in its most general form so that it incorporates Doppler broadening, arbitrary level detunings, and arbitrary decay rates, a numerical analysis is required to investigate DFWM. To develop an analytical approach, we ignore Doppler broadening in the following and assume that the laser frequency ω is coincident with the one-photon transition frequency ω_a . Dispersive effects are, however, included by allowing Zeeman splitting of the ground-state sublevels in the presence of an applied magnetic field. The inclusion of Zeeman splitting makes it possible to investigate level-crossing resonance^{18–23} in DFWM spectra that may find application in high-resolution spectroscopy.

For the sake of generality, no severe restrictions are imposed on the population decay rates γ_i and the coherence decay rates γ_{ij} ($i, j = 0, 1$, and 2) except for assuming that

$\gamma_1 = \gamma_2$ and $\gamma_{01} = \gamma_{02}$ because of the nearly degenerate nature of the ground-state Zeeman sublevels. The effect of phase-perturbing collisions on the coherence decay rates is allowed by assuming

$$\gamma_{ij} = (\gamma_i + \gamma_j)/2 + \gamma_{ij}^{ph}, \quad (12)$$

where γ_{ij}^{ph} is the collisional decay rate. It should, however, be mentioned that the introduction of an effective dephasing rate for Zeeman coherence is an approximation.¹⁸ The pressure dependence of the population decay rates γ_i can be easily included.

With the above-mentioned simplifications it is possible to obtain, without further approximations, the following analytical nonperturbative expression for the medium susceptibilities χ_1 and χ_2 corresponding to σ_+ and σ_- polarizations, respectively (see the Appendix for details):

$$\chi_n = \frac{2\alpha_{n0}}{kD} \frac{\pm\delta + i}{1 + \delta^2} \left[1 + \frac{(p \pm i\delta r)I'_{3-n}}{(1+p+\bar{I}) \pm i\delta(1+r+\bar{I})} \right], \quad (13)$$

where upper or lower sign is chosen for $n=1$ and $n=2$, respectively. The saturation denominator D is given by

$$D = 1 + (1+q)(I'_1 + I'_2) + (1+2q)I'_1I'_2 \left[\frac{p(1+p+\bar{I}) + \delta^2(p+p\bar{I}+r^2)}{(1+p+\bar{I})^2 + \delta^2(1+r+\bar{I})^2} \right] \quad (14)$$

and we have introduced the following dimensionless parameters:

$$\delta = \frac{\Omega_{12}}{2\gamma_{01}}, \quad p = \frac{\gamma_{12}^{ph}}{\gamma_1}, \quad q = \frac{\gamma_1}{\gamma_0}, \quad (15)$$

$$r = \left[\frac{2\gamma_{01}}{\gamma_1} - 1 \right] = \frac{1}{q} + \frac{2\gamma_{01}^{ph}}{\gamma_1}, \quad (16)$$

$$I'_n = \frac{I_n}{1 + \delta^2}, \quad I_n = \frac{|A_n|^2}{I_{sn}}, \quad \bar{I} = \frac{1}{2}(I'_1 + I'_2). \quad (17)$$

The saturation intensity

$$I_{sn} = 2q(\hbar^2\gamma_0\gamma_{0n}/|\mu_{0n}|^2) \quad (18)$$

and the resonant unsaturated field-absorption coefficient

$$\alpha_{n0} = N|\mu_{0n}|^2 f_0 \omega / (2\epsilon_0 \hbar c \gamma_{0n}) \quad (19)$$

have different values for the left and right circular polarizations if the corresponding transition dipole moments are different. Here N is the atomic density, f_0 is the fractional population of a sublevel, and Ω_{12} is the frequency separation of the Zeeman sublevels. The parameter δ is a measure of the Zeeman splitting in units of the homogeneous line width γ_{01} . The relaxation-rate ratio $q = \gamma_1/\gamma_0$ plays an important role. If the degenerate lower level corresponds to the system ground state, it is expected that $q \ll 1$. Since the saturation intensity I_{sn} scales linearly with q , a three-level system in this specific case saturates at much lower pump intensities compared to those required for a two-level system.²⁶ The collisional decay of Zeeman coherence is governed by the parameter

$p = \gamma_{12}^{pb} / \gamma_1$ while the parameter $r \geq q^{-1}$ defined by Eq. (16) takes into account collisional dipole dephasing.

Using third-order perturbation theory, Lam and Abrams¹³ have identified three distinct grating mechanisms for DFWM which they term the normal-population, the cross-population, and the Zeeman-coherence mechanisms. It is of interest to identify the contribution of each mechanism in the nonperturbative treatment presented here. To the lowest order in pump intensities I_1 and I_2 , the susceptibility χ_1 from Eq. (13) takes the form

$$\chi_1 \approx \frac{2\alpha_{10}}{k} \frac{\delta + i}{(1 + \delta^2)^2} \left[1 + \delta^2 - (q + 1)I_1 - \left[q + \frac{1 + i\delta}{1 + p + i\delta(1 + r)} \right] I_2 \right]. \quad (20)$$

The self-saturation term $(q + 1)I_1$ is related to the normal-population mechanism and for the polarization configuration of Fig. 1 it does not contribute to DFWM. The cross-saturation term has two separate origins. The term proportional to qI_2 arises from the cross-population mechanism while the other is related to the Zeeman-coherence mechanism. Since $q = \gamma_1 / \gamma_0$ can be much less than unity, the Zeeman-coherence contribution to DFWM usually dominates. The nonlinear coupling coefficient κ_{43} , responsible for the conjugate-wave generation, can be obtained using Eqs. (9c) and (20) and is given by

$$|\kappa_{43}| = \frac{\alpha_{10}(I_1 I_2)^{1/2}}{(1 + \delta^2)} \left| \frac{q(\delta + i)}{(1 + \delta^2)} + \frac{\delta(1 + r) + i(1 + p)}{(1 + p)^2 + \delta^2(1 + r)^2} \right|. \quad (21)$$

It is easy to verify that, within the framework of third-order perturbation theory, the coupling is maximum for $\delta = 0$. It will be seen in Sec. IV that when the saturation effects are included, the DFWM response peaks at $\delta \approx q^{-1}$. Equation (21) clearly shows the two contributions to the coupling coefficient. The term proportional to q is due to the cross-population mechanism while the last term arises from the Zeeman-coherence mechanism.

IV. REFLECTIVITY BEHAVIOR

In this section we investigate the dependence of the phase-conjugate reflectivity R on various parameters of interest. To illustrate the main qualitative features of the reflectivity behavior in a transparent manner, we assume that the small-signal absorption coefficient is the same for opposite circular polarizations and set $\alpha_{10} = \alpha_{20} \equiv \alpha_0$. Furthermore, in this section we restrict ourselves to the case of equal-intensity pump waves and take $I_1 = I_2 \equiv I_p$. We also ignore collisional dipole dephasing so that $r = 1/q$ from Eq. (16). In the following we choose $\alpha_0 L = 5$.

Figure 2 shows the variation of the reflectivity R with the pump intensity I_p for several values of q and δ after choosing $p = 0$. For finite values of p , the collisional decay of Zeeman coherence reduces R in magnitude but the

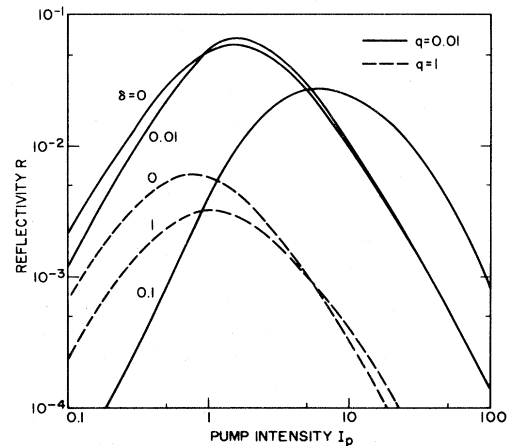


FIG. 2. Variation of the phase-conjugate reflectivity R with the pump intensity I_p (normalized to the saturation intensity) for several values of the Zeeman-splitting parameter δ . The parameter q denotes the ratio of lower to upper level relaxation rates.

qualitative behavior remains unchanged. The reflectivity curves are reminiscent of a similar behavior observed for a two-level system.³ The reflectivity peaks when the pump intensity is of the order of saturation intensity ($I_p \sim 1$) and decreases with the further increase of I_p owing to the saturation effects. We note that higher values of R are obtained at lower values of pump intensities when $q \ll 1$ (the saturation intensity scales linearly with q). This is often the case, in practice, if the lower atomic state corresponds to the system ground state. Dispersive effects are manifested in Fig. 1 through finite values of δ arising from the Zeeman splitting. In general, as δ increases, the reflectivity peak decreases in height and shifts towards higher values of the pump intensity. However, when $q \ll 1$, the maximum reflectivity R is obtained for $\delta \neq 0$, indicating the importance of saturated dispersion in three-level systems.

From the viewpoint of spectroscopic applications, it is of considerable interest to investigate detailed features of reflectivity spectra obtained by recording the DFWM response as a function of the Zeeman-splitting parameter δ . Since DFWM provides yet another nonlinear technique to probe a three-level system, a narrow central resonance might be expected to occur under appropriate conditions.

The literature is vast¹⁹⁻²⁷ on the subject of narrow nonlinear resonances in three-level systems and many different nonlinear techniques (resonance fluorescence, probe absorption, stimulated Raman scattering, mode crossing, level crossing, etc.) have been employed. More closely related to the present work is, however, the technique of polarization spectroscopy²⁷ where subnatural linewidths have been obtained^{28,29} by probing Zeeman sublevels.

The DFWM configuration shown in Fig. 1 does not appear to have been used previously to investigate the level-crossing resonance. It is important to note that the laser frequency is kept fixed here and the phase-conjugate spectrum is obtained by varying the Larmor frequency (using an axial magnetic field) associated with the Zeeman sublevels. In what follows we study power and collisional

broadening of the level-crossing resonance. It should be mentioned that, in general, collisions affect all relaxation rates and the analysis is capable of incorporating pressure effects through the parameters p , q , and r defined by Eqs. (15) and (16). For the sake of illustration we simplify the situation by assuming that only γ_{12} is modified by phase-perturbing collisions. This is qualitatively justified since Zeeman coherence plays an essential role in producing the level-crossing resonance.

The level-crossing reflectivity spectrum is shown in Fig. 3 for several values of the pump intensities I_p after choosing $p=0$ and $q=0.01$. A dip at $\delta=0$ starts to form when $I_p \approx 1$ and becomes deeper and wider as I_p increases further. Power broadening of the zero-field narrow resonance is clearly seen in Fig. 3. To illustrate that Zeeman coherence plays an important role in dip formation, Fig. 4 shows the reflectivity spectra at a fixed pump intensity for several values of $p = \gamma_{12}^{ph}/\gamma_1$. As p increases, the collisional decay of Zeeman coherence decreases the DFWM signal and introduces collisional broadening of the zero-field resonance.

In Figs. 3 and 4 the relaxation-rate ratio $q = \gamma_1/\gamma_0$ was chosen to be small so that, as discussed in Sec. III, the Zeeman-coherence contribution to DFWM dominated in comparison to the cross-population contribution. In order to discuss the relative importance of these two mechanisms to DFWM, Fig. 5 shows the reflectivity spectra for several values of q at a fixed normalized pump intensity $I_p=2$. It should be stressed that the saturation intensity scales linearly with q so that the actual pump intensity decreases as q is lowered. The most notable feature of Fig. 5 is that a central narrow peak occurring for $q \sim 1$ is replaced by a central narrow dip when $q \ll 1$. This qualitative change is a result of competition between the Zeeman-coherence and the cross-population contributions to DFWM and can be explained as follows. The cross-population and the Zeeman-coherence mechanisms con-

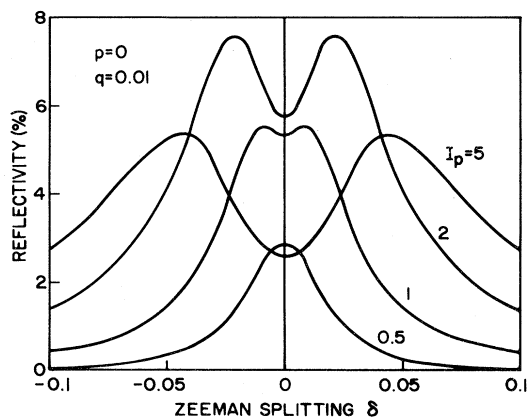


FIG. 3. Phase-conjugate reflectivity spectrum obtained by varying the Zeeman-splitting parameter δ (the sublevel-frequency separation in units of the homogeneous linewidth). In the saturation regime ($I_p \approx 1$) a narrow central resonance related to transverse optical pumping occurs and its width exhibits power broadening with further increase in the pump intensity.

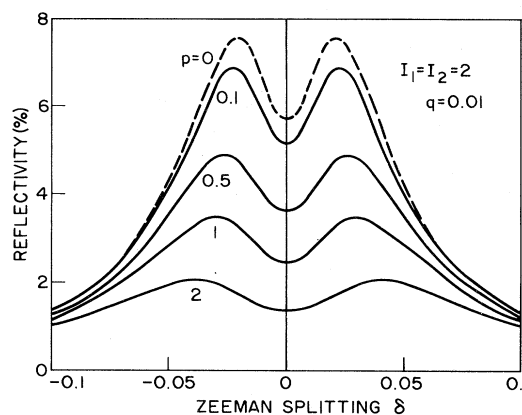


FIG. 4. Effect of dephasing collisions on the level-crossing reflectivity spectrum at a fixed pump intensity. The parameter p is a measure of the collision-induced increase in the Zeeman-coherence relaxation rate.

tribute to DFWM in such a way that the former contribution peaks at $\delta=0$ while the latter peaks at $\delta \approx \pm q$. The relative strength of their contributions varies with q and as q decreases the Zeeman-coherence contribution dominates over that of cross-population. Furthermore, the two contributions add in phase only when $\delta=0$ [see Eq. (21)]. The qualitative features shown in Fig. 5 arise from a superposition of these different contributions. The collisional decay of Zeeman coherence is ignored in Fig. 5 by setting $p=0$. However, finite values of p do not change the qualitative behavior except for dip broadening shown in Fig. 4.

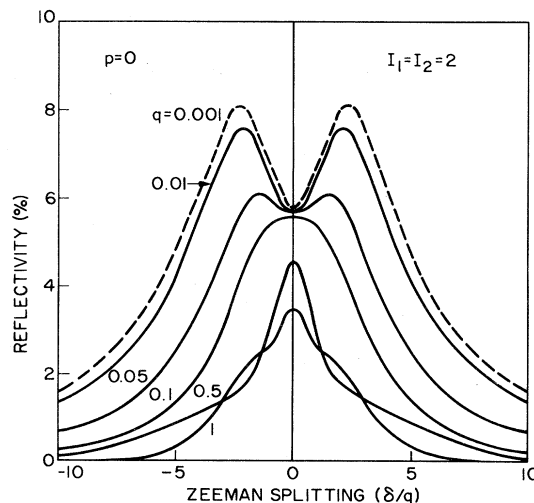


FIG. 5. Phase-conjugate reflectivity spectrum at a fixed pump intensity for several values of the parameter q defined as the ratio of lower to upper level relaxation rates. The narrow level-crossing resonance manifests as a central peak for $q \sim 1$ and as a central dip for $q \ll 1$.

V. POLARIZATION ANISOTROPY IN PHASE CONJUGATION

In the previous discussion, based on the geometry shown in Fig. 1, the forward pump and the probe waves are taken to be orthogonally circularly polarized. Since the generated wave has a polarization conjugate to that of the probe, this process is termed vectorial phase conjugation. Recently, several authors have discussed the use of mutually orthogonal circularly polarized pump beams for the generation of phase-conjugate vector wave fronts.⁷⁻¹² Since an arbitrary probe polarization can be expressed as a superposition of σ_+ and σ_- polarizations, it is sufficient to supplement the present analysis by considering the opposite case wherein the forward pump and probe waves are copolarized.

For the specific case of σ_+ polarization of E_1 and E_3 fields, one can follow an analysis analogous to that of Sec. II, where now $E'_1 = E_1 + E_3$ and $E'_2 = E_2 + E_4$ in Eqs. (2)–(5). The phase-conjugate reflectivity R' is still given by Eq. (10) but the definitions of α_3 and α_4 , as well as that of κ_{34} and κ_{43} [see Eq. (9)], are interchanged. Using a simple symmetry argument, it is straightforward to establish that

$$R'(I_1, I_2) \equiv R(I_2, I_1). \quad (22)$$

A change of probe polarization from σ_- to σ_+ is equivalent to, as far as the DFWM response is concerned, an interchange of pump intensities (keeping the probe polarization fixed). It follows immediately that a sufficient condition for vectorial phase conjugation is to ensure equal intensities for the counterpropagating pump waves. We hasten to add that this conclusion is based on the assumption that depletion and absorption of the pump waves are negligible.

In the more general case of unequal pump intensities ($I_1 \neq I_2$), $R' = R$ if R is a symmetric function of I_1 and I_2 . Calculations show that this is indeed the case when $\delta = 0$, i.e., when the Zeeman sublevels are degenerate. The inclusion of dispersive effects for $\delta \neq 0$ introduces polarization anisotropy. This behavior is illustrated in Fig. 6 where the reflectivity spectrum is shown for several pump intensities. The choice of $p = 0$ and $q = 0.01$ implies that the DFWM response arises mainly from the Zeeman-coherence mechanism. Dashed curves are obtained by interchanging the values of I_1 and I_2 . Alternatively, the dashed curves correspond to a change of probe polarization from σ_- to σ_+ while keeping the pump intensities unchanged. An inspection of Fig. 6 shows that in a narrow range $0 < \delta \leq 0.1$, the DFWM response is markedly anisotropic with respect to the probe polarization. From a spectroscopic viewpoint this result implies that, if $I_1 > I_2$, the central resonance in DFWM due to level crossing is sharper when the forward pump and the probe waves have orthogonal circular polarizations.

VI. DISCUSSION AND CONCLUSIONS

In this paper we have presented a nonperturbative theory of phase conjugation through DFWM on homogeneously broadened coupled transitions. The pump

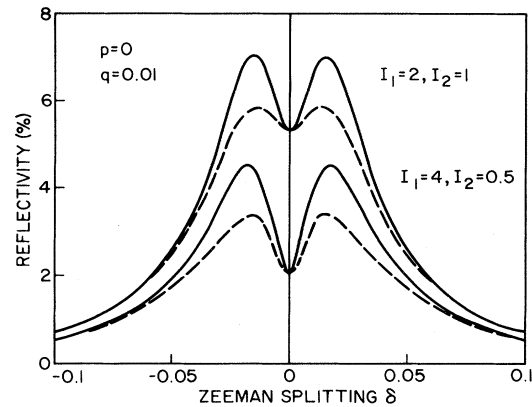


FIG. 6. Illustration of the polarization anisotropy in the level-crossing reflectivity spectrum in the presence of pump imbalance. The solid line curves correspond to the polarization configuration of Fig. 1 (probe is σ_- polarized). The dashed-line curves are obtained by changing the probe polarization from σ_- to σ_+ .

waves are assumed to have orthogonal circular polarizations and interact with different one-photon transitions sharing a common upper level. This choice of pump polarizations avoids spatial hole-burning and generates wave fronts that are conjugate including the sense of polarization. The probe polarization can be either identical or orthogonal to that of the forward pump. Although both cases have been discussed, particular attention is paid to the case of orthogonal polarization since it permits the use of collinear DFWM geometry.

Using a Λ -type three-level model for the nonlinear medium, it is shown that Zeeman coherence, arising from the two-photon coupling of the lower-state sublevels, plays an important and usually dominant role in producing DFWM response. One of the main conclusions drawn from an inspection of Fig. 2 is that under certain conditions significant ($\sim 10\%$) values of phase-conjugate reflectivities can be obtained at pump intensities much lower than those required for a two-level system. Two requirements for a high DFWM response are (i) that the collisional relaxation of Zeeman coherence should be negligible and (ii) the upper state should relax much faster than the degenerate lower state. The latter conditions is readily satisfied, in practice, if the lower state corresponds to the system ground state. The effective ground-state lifetime is then governed by the radiation-atom interaction time.

For the sake of analytical simplicity, the present analysis has assumed that the laser frequency is coincident with the one-photon-transition frequency. Similar to a two-level system,³ higher values of the phase-conjugate reflectivity can be expected if the laser-detuning effects are included in the analysis. Their inclusion will, however, require a numerical treatment in the saturation regime considered here. It may be remarked that the laser-detuning effects are essential for the discussion of so-called pressure-induced extra resonance in four-wave mixing (PIER4).³⁰⁻³²

Keeping in mind spectroscopic applications, the level-crossing DFWM spectrum is particularly studied. Here the spectral response is obtained by varying the Larmor frequency (through an axial magnetic field) associated with the Zeeman splitting and its main qualitative features are shown in Figs. 3–6. The main conclusion is that the DFWM spectrum exhibits a narrow zero-field resonance that manifest either as a dip or a peak depending on various relaxation rates (see Fig. 5). The width of the resonance is related to the Zeeman-coherence decay rate and can be much less than the homogeneous line width. The physical origin of this resonance lies in a phenomenon termed coherent population trapping, also referred to as transverse optical pumping.²² It is important to stress that both optical pumping and saturation are required to produce subnatural linewidth features.²⁶

The present analysis can readily be extended to include the case where the upper state is degenerate in lieu of the lower one. The nonlinear medium is now modeled in terms of a V -type three-level system. The susceptibility can be obtained with only minor modifications of the density-matrix solution given in the Appendix. Following the prescription of Feld and Javan,²⁰ one may show that the susceptibility is still given by Eq. (13) if we change the sign of the Zeeman-splitting parameter δ . Since the phase-conjugate reflectivity is an even function of δ , one may use the results directly even for a V -type system provided appropriate values of the parameters are used. The parameter whose value is most affected is q defined as the ratio of the degenerate- to nondegenerate-state relaxation rate. For a V -type system, the relevant values of this parameter are $q \geq 1$ because of the allowed radiative decay of the upper state. Several conclusions can now be drawn from an inspection of Figs. 2 and 5. The DFWM response will be weaker and will require higher pump intensities when compared to a Λ -type system. The most notable qualitative change will occur in the level-crossing DFWM spectrum that is predicted to exhibit a narrow central peak.

In an attempt to present the saturation effects analytically, Doppler broadening has been neglected in the present work. For the case of DFWM in atomic vapors, atomic-motion effects may be important unless a well-collimated atomic beam is used for experiments. In a recent work, Doppler effects were considered assuming that only one of the pump beams is above the saturation threshold.³³ For the important case of two saturating pump beams, the inclusion of Doppler broadening will require an extensive numerical analysis that, in principle, can be carried out using the density-matrix formalism^{18–24} (see the Appendix). A qualitative understanding of Doppler effects can be achieved in terms of an often-used grating analogy.^{10–13} The atomic motion will lead to a washout of the cross-population grating generated by backward-pump and probe interference while the Zeeman-coherence *tensor* grating will be relatively unaffected. The DFWM signal will then solely arise from the Zeeman-coherence mechanism and the main qualitative features of Figs. 2–6 should remain largely unaffected. Experiments performed using sodium vapor^{9–11} have con-

firmed the minor role played by the population gratings in such systems. We should, however, stress that these conclusions hold only for a nearly collinear DFWM geometry.¹²

It may be worthwhile to point out the essential differences between the present model and a previous model²² used in high-resolution spectroscopy. The model of Ref. 22 considers a closed three-level system that amounts to assuming that atoms do not leave the interaction region. The only allowed decay mechanism for the ground-state sublevels is a slow (usually \sim few ms) collisional population transfer that tends to equalize the sublevel populations. In a typical experimental situation, however, atomic motion or collisional diffusion tends to move atoms outside the beam cross-section on a faster time scale (\sim few μ s) so that it is more appropriate to consider an open three-level system. (Of course, the average atomic density remains constant since the same mechanism brings other atoms inside the interaction region.) Note that even though no direct population transfer is involved, the net effect is to indirectly equalize sublevel populations. Finite interaction time provides an effective ground-state lifetime^{26,34} and should be incorporated for a realistic description of the experimental situation. The relaxation scheme of the present model is general enough to include this effect. Furthermore, since no constraints are imposed on the four independent relaxation rates γ_0 , γ_1 , γ_{01} , and γ_{12} , pressure effects can be readily included.³⁵ We feel that the analytic expression (13) developed in this paper should be useful in discussing a variety of nonlinear phenomena such as optical bistability, phase conjugation, and two-mode lasing in Zeeman lasers.

An experimental verification of the theoretical predictions reported here would be of considerable interest. Although several experiments have been performed using sodium vapor for DFWM,^{9–11} spectroscopic features were probed by varying the laser frequency. Level-crossing spectroscopy with the geometry of Fig. 1 appears to have attracted little attention. Recently, the D_1 absorption line of sodium was used to record³⁶ the DFWM spectrum by varying the external magnetic field at a fixed laser frequency. Even though the present analysis is not directly available due to a different polarization scheme adopted for the experiment, the level-crossing spectrum exhibited all the qualitative features shown in Fig. 3. In accordance with our theory, a narrow central dip with a subnatural spectral width of ~ 1 MHz (the optical homogeneous linewidth was ~ 2 GHz) was clearly observed when the pump intensity exceeded the three-level saturation threshold.

An example of the atomic system, where a three-level system is readily realized and our analysis is directly applicable, is provided by samarium vapor with the one-photon resonance $6s^2 7F_1 \rightarrow 6s 6p 7F_0$ at 570.7-nm wavelength. Significant DFWM response is expected at a pump power of several milliwatts. An important class of materials for DFWM is related to ion-doped crystals. This will eliminate Doppler broadening although the one-photon transition may still be inhomogeneously broadened due to crystal inhomogeneities.

ACKNOWLEDGMENTS

The author is thankful to Jürgen Mlynek for useful discussion and for communicating the experimental results before publication.

APPENDIX: SUSCEPTIBILITY
FOR A THREE-LEVEL SYSTEM INTERACTING
WITH TWO INTENSE OPTICAL FIELDS

A three-level system interacting with two optical fields has been extensively studied^{20–25} in the context of high-resolution spectroscopy. Although most of the work^{20,25} assumed one of the fields to be weak, more recently the case of two arbitrarily intense optical fields has been considered.^{21–24} We shall follow the treatment of Ref. 24 since it is applicable for arbitrary relaxation rates.

In the density-matrix formalism the equation of motion $i\hbar\dot{\rho}=[H,\rho]$ for the density operator ρ is used to obtain a set of nine coupled equations for the matrix elements $\rho_{ij}=\langle i|\rho|j\rangle$, where $i,j=0,1$, and 2 corresponding to the three levels shown in Fig. 1. Here

$$H=H_0+V=H_0-\vec{\mu}\cdot\vec{E}, \quad (\text{A1})$$

where H_0 is the system Hamiltonian in the absence of the optical fields, $\vec{\mu}$ is the dipole-moment operator and the total electric field

$$\vec{E}=\frac{1}{2}(E_1\hat{e}_R+E_2\hat{e}_L)e^{-i\omega t}+\text{c.c.} \quad (\text{A2})$$

Using phenomenological decay rates γ_i and γ_{ij} for the diagonal and off-diagonal matrix elements ρ_{ii} and ρ_{ij} , respectively, the density-matrix equations are (see Fig. 1 for the level scheme)

$$\dot{\rho}_{00}+\gamma_0(\rho_{00}-\bar{\rho}_{00})=(i\hbar)^{-1}(V_{01}\rho_{10}+V_{02}\rho_{20}-\text{c.c.}), \quad (\text{A3})$$

$$\dot{\rho}_{11}+\gamma_1(\rho_{11}-\bar{\rho}_{11})=(i\hbar)^{-1}(V_{10}\rho_{01}-\rho_{10}V_{01}), \quad (\text{A4})$$

$$\dot{\rho}_{22}+\gamma_2(\rho_{22}-\bar{\rho}_{22})=(i\hbar)^{-1}(V_{20}\rho_{02}-\rho_{20}V_{02}), \quad (\text{A5})$$

$$\dot{\rho}_{01}+\gamma_{01}\rho_{01}=(i\hbar)^{-1}[\hbar\Omega_{01}\rho_{01}+V_{01}(\rho_{11}-\rho_{00})+V_{02}\rho_{21}], \quad (\text{A6})$$

$$\dot{\rho}_{02}+\gamma_{02}\rho_{02}=(i\hbar)^{-1}[\hbar\Omega_{02}\rho_{02}+V_{02}(\rho_{22}-\rho_{00})+V_{01}\rho_{12}], \quad (\text{A7})$$

$$\dot{\rho}_{21}+\gamma_{21}\rho_{21}=(i\hbar)^{-1}(\hbar\Omega_{12}\rho_{21}+V_{20}\rho_{01}-V_{01}\rho_{20}), \quad (\text{A8})$$

where $\bar{\rho}_{nn}$ is the equilibrium population for the level $|n\rangle$, Ω_{ij} is the atomic transition frequency,

$$V_{0n}=-(\mu_{0n}E_n/2)e^{-i\omega t},$$

$$\mu_{01}=\langle 0|\vec{e}_R\cdot\vec{\mu}|1\rangle,$$

$$\mu_{02}=\langle 0|\hat{e}_L\cdot\vec{\mu}|2\rangle,$$

and the terms involving V_{12} have been neglected since the corresponding transition is dipole forbidden. The quadrupole coupling of the sublevels is, however, included through Zeeman coherence ρ_{21} .

The induced polarization can be separated into two

parts corresponding to different circular polarizations,

$$\vec{P}=N\text{Tr}(\vec{\mu}\rho)=N(\hat{e}_R\mu_{10}\rho_{01}+\hat{e}_L\mu_{20}\rho_{02})+\text{c.c.} \quad (\text{A9})$$

Its comparison with

$$\vec{P}=\frac{1}{2}\epsilon_0(\chi_1E_1\hat{e}_R+\chi_2E_2\hat{e}_L)e^{-i\omega t}+\text{c.c.} \quad (\text{A10})$$

leads to the following expression for the susceptibility:

$$\chi_n=\frac{2N\mu_{n0}}{\epsilon_0E_n}\rho_{0n}e^{i\omega t}. \quad (\text{A11})$$

Here ϵ_0 is the vacuum permittivity and N is the atomic density.

Owing to the resonant nature of matter-radiation interaction a nearly exact steady-state solution of the density-matrix equations (A3)–(A8) can be obtained by assuming $\rho_{0n}=\bar{\rho}_{0n}\exp(-i\omega t)$ and setting all time derivatives to be zero. The resulting set of algebraic equations can be solved without further approximations.²⁴ Using the final result in Eq. (A11) we obtain

$$\chi_1=\frac{|\mu_{10}|^2}{\epsilon_0\hbar}\frac{|\beta|^2r_{20}+(RL_2-|\alpha|^2)r_{10}}{L_1|\alpha|^2+L_2|\beta|^2-L_1L_2R}, \quad (\text{A12})$$

$$\chi_2^*=-\frac{|\mu_{20}|^2}{\epsilon_0\hbar}\frac{|\alpha|^2r_{10}+(RL_1-|\alpha|^2)r_{20}}{L_1|\alpha|^2+L_2|\beta|^2-L_1L_2R}, \quad (\text{A13})$$

where the population differences are given by

$$r_{10}=\frac{(1-J_{bb})\bar{r}_{10}+J_{ab}\bar{r}_{20}}{(1-J_{aa})(1-J_{bb})-J_{ab}J_{ba}}, \quad (\text{A14})$$

$$r_{20}=\frac{(1-J_{aa})\bar{r}_{20}+J_{ba}\bar{r}_{10}}{(1-J_{aa})(1-J_{bb})-J_{ab}J_{ba}} \quad (\text{A15})$$

with

$$J_{ij}=2\text{Im}(C_{ij}), \quad (i,j=a,b) \quad (\text{A16})$$

$$C_{aa}=\frac{|\alpha|^2}{\gamma_0N}\left[\frac{2\gamma_{01}}{\gamma_1}(L_2R-|\alpha|^2)+|\beta|^2\right], \quad (\text{A17})$$

$$C_{bb}=\frac{|\beta|^2}{\gamma_0N}\left[\frac{2\gamma_{02}}{\gamma_2}(L_1R-|\beta|^2)+|\alpha|^2\right], \quad (\text{A18})$$

$$C_{ab}=\frac{|\beta|^2}{\gamma_0N}\left[\frac{2\gamma_{01}}{\gamma_1}|\alpha|^2+(L_1R-|\beta|^2)\right], \quad (\text{A19})$$

$$C_{ba}=\frac{|\alpha|^2}{\gamma_0N}\left[\frac{2\gamma_{02}}{\gamma_1}|\beta|^2+(L_2R-|\alpha|^2)\right], \quad (\text{A20})$$

$$N=L_1L_2R-L_1|\alpha|^2-L_2|\beta|^2. \quad (\text{A21})$$

In writing (A12)–(A21) we have used the following notations:

$$\alpha=(\mu_{10}E_1^*/2\hbar), \quad \beta=(\mu_{02}E_2/2\hbar), \quad (\text{A22})$$

$$r_{n0}=(\rho_{nn}-\rho_{00}), \quad \bar{r}_{n0}=(\bar{\rho}_{nn}-\bar{\rho}_{00}), \quad (\text{A23})$$

$$L_1=\omega-\Omega_{01}+i\gamma_{01}, \quad (\text{A24})$$

$$L_2=\Omega_{02}-\omega+i\gamma_{02}, \quad (\text{A25})$$

$$R=\Omega_{12}+i\gamma_{12}. \quad (\text{A26})$$

The three-level system is assumed to be homogeneously broadened. Doppler broadening can be incorporated²⁰ by redefining the complex frequency detunings L_1 , L_2 , and R .

The analysis is considerably simplified if we assume $\Omega_{01} = \omega_a - \omega_L$, $\Omega_{02} = \omega_a + \omega_L$, and exact resonance $\omega = \omega_a$. Here ω_a is the transition frequency and $\omega_L = \frac{1}{2}\Omega_{12}$ is the Larmor frequency due to Zeeman splitting. We further assume $\gamma_1 = \gamma_2$ and $\gamma_{01} = \gamma_{02}$. Using Eqs. (A24) and (A25),

$$L_1 = L_2 \equiv L = i\gamma_{01}(1 - i\delta), \quad (\text{A27})$$

where $\delta = \Omega_{12}/2\gamma_{01}$ is a dimensionless measure of the Zeeman splitting. We now introduce the following dimensionless quantities:

$$p = \gamma_{12}^{ph}/\gamma_1, \quad q = \gamma_1/\gamma_0, \quad (\text{A28})$$

$$r = (2\gamma_{01}/\gamma_1 - 1) = q^{-1} + 2\gamma_{01}^{ph}/\gamma_1, \quad (\text{A29})$$

$$I_1 = 2|\alpha|^2/(\gamma_1\gamma_{01}) = |E_1|^2/I_{s1}, \quad (\text{A30})$$

$$I_2 = 2|\beta|^2/(\gamma_2\gamma_{02}) = |E_2|^2/I_{s2}, \quad (\text{A31})$$

where γ_{ij}^{ph} is defined by Eq. (12) and I_{sn} is a measure of saturation intensity for the three-level system ($n=1,2$). Equations (A16)–(A21) then yield

$$J_{aa} = -(q+1)I_1' + J_0, \quad (\text{A32})$$

$$J_{bb} = -(q+1)I_2' + J_0, \quad (\text{A33})$$

$$J_{ba} = -qI_1' + J_0, \quad (\text{A34})$$

$$J_{ab} = -qI_2' + J_0, \quad (\text{A35})$$

where the two-photon term $J_0 = (q + \frac{1}{2})QI_1'I_2'$ with

$$Q = \frac{(1+p+\bar{I}) + \delta^2(1+2r-p+\bar{I})}{(1+p+\bar{I})^2 + \delta^2(1+r+\bar{I})^2}, \quad (\text{A36})$$

$$I_n' = I_n/(1+\delta^2), \quad \bar{I} = (I_1' + I_2')/2. \quad (\text{A37})$$

Using Eqs. (A32)–(A35) in Eqs. (A14) and (A15), the population differences are given by

$$r_{n0} = (f_0/D)(1 + I_{3-n}'), \quad n=1,2 \quad (\text{A38})$$

where $f_0 = \bar{r}_{10} = \bar{r}_{20}$ and the saturation denominator

$$D = 1 + (q+1)(I_1' + I_2') + (2q+1)[1 - Q(1+\bar{I})]I_1'I_2'. \quad (\text{A39})$$

Note the presence of self-saturation, cross saturation, and two-photon saturation. The two terms on the right-hand side of Eq. (A38) can be attributed to one- and two-photon transitions, respectively. The quantity f_0 represents the fractional population assumed to be the same for each sublevel ($f_0 = \frac{1}{3}$). This is not a limitation since the Boltzmann factor $\hbar\Omega_{12}/k_B T \lesssim 10^{-6}$ and all sublevels are equally populated (in the absence of applied fields) to one part in a million. Substitution of Eq. (A38) in Eqs. (A12) and (A13) yields the final expression for χ_n given by Eq. (13) of Sec. III.

¹For a recent review and an extensive bibliography, see D. M. Pepper, *Opt. Eng.* **21**, 156 (1982); *Optical Phase Conjugation*, edited by R. A. Fisher (Academic, New York, 1983).

²M. Ducloy, in *Festkörperprobleme*, edited by J. Treusch (Vieweg, Braunschweig, 1982), Vol. XXII, p. 35.

³R. L. Abrams and R. C. Lind, *Opt. Lett.* **2**, 94 (1978); **3**, 205(E) (1978).

⁴R. C. Lind, D. G. Steel, and G. J. Dunning, *Opt. Eng.* **21**, 190 (1982) and references cited therein.

⁵G. P. Agrawal, A. Van Lerberghe, P. Aubourg, and J. L. Boulnois, *Opt. Lett.* **7**, 540 (1982).

⁶J. Nilsen and A. Yariv, *IEEE J. Quantum Electron.* **QE-18**, 1947 (1982).

⁷B. Ya Zel'dovich and V. V. Shkunov, *Kvant. Elektron. (Moscow)* **6**, 629 (1979) [*Sov. J. Quantum Electron.* **2**, 379 (1979)].

⁸G. Martin, L. K. Lam, and R. W. Hellwarth, *Opt. Lett.* **5**, 185 (1980).

⁹S. Saikan and M. Kiguchi, *Opt. Lett.* **7**, 555 (1982).

¹⁰J. F. Lam, D. G. Steel, R. A. McFarlane, and R. C. Lind, *Appl. Phys. Lett.* **38**, 977 (1981).

¹¹S. N. Jabr, L. K. Lam, and R. W. Hellwarth, *Phys. Rev. A* **24**, 3264 (1981).

¹²D. Bloch and M. Ducloy, *J. Phys. B* **14**, L471 (1981).

¹³J. F. Lam and R. L. Abrams, *Phys. Rev. A* **26**, 1539 (1982).

¹⁴G. P. Agrawal, *IEEE J. Quantum Electron.* **QE-17**, 2335 (1981); *J. Opt. Soc. Am.* **73**, 654 (1983).

¹⁵G. P. Agrawal, *Opt. Lett.* **8**, 359 (1983); Proceedings of the Fifth Rochester Conference on Coherence and Quantum Optics, Rochester, New York, June 1983 (in press).

¹⁶In the pulsed case the analysis developed here is still applicable if the pulse duration of the pump and probe waves is much longer than the medium response time.

¹⁷G. P. Agrawal, *Opt. Commun.* **42**, 366 (1982).

¹⁸A. Omont, *Prog. Quantum Electron.* **5**, 69 (1977).

¹⁹B. Decomps, M. Dumont, and M. Ducloy, in *Laser Spectroscopy of Atoms and Molecules*, edited by H. Walther (Springer, Heidelberg, 1976) Vol. 2.

²⁰M. S. Feld and A. Javan, *Phys. Rev.* **177**, 540 (1969).

²¹R. G. Brewer and E. L. Hahn, *Phys. Rev. A* **11**, 1641 (1975).

²²G. Orriols, *Nuovo Cimento B* **53**, 1 (1979).

²³A. V. Kats, V. M. Kontorovich, and A. V. Nikolaev, *Zh. Eksp. Teor. Fiz.* **78**, 1696 (1980) [*Sov. Phys.—JETP* **51**, 851 (1980)].

²⁴J. Heppner, C. O. Weiss, U. Hübner, and G. Schinn, *IEEE J. Quantum Electron.* **QE-16**, 392 (1980).

²⁵V. S. Letokhov and V. P. Chebotayev, *Nonlinear Laser Spectroscopy* (Springer, Berlin, 1977).

²⁶D. E. Murnick, M. S. Feld, M. M. Burns, T. V. Kühn, and P. G. Pappas, in *Laser Spectroscopy IV*, edited by H. Walther and K. W. Rothe (Springer, Heidelberg, 1979), p. 195.

²⁷C. Wieman and T. W. Hänsch, *Phys. Rev. Lett.* **36**, 1170 (1976).

- ²⁸J. Mlynek, K. H. Drake, G. Kersten, D. Frölich, and W. Lange, *Opt. Lett.* **6**, 87 (1981).
- ²⁹W. Gawlik, J. Kowalski, F. Träger, and M. Vollmer, *Phys. Rev. Lett.* **48**, 871 (1982).
- ³⁰Y. Prior, A. R. Bogdan, M. Dagenais, and N. Bloembergen, *Phys. Rev. Lett.* **46**, 111 (1981).
- ³¹M. Dagenais, *Phys. Rev. A* **26**, 869 (1982).
- ³²F. A. M. de Olivera, C. B. de Araujo, and J. R. Rios Leite, *Phys. Rev. A* **25**, 2430 (1982).
- ³³D. Bloch and M. Ducloy, *J. Opt. Soc. Am.* **73**, 635 (1983).
- ³⁴J. E. Thomas and W. W. Quivers, Jr., *Phys. Rev. A* **22**, 2115 (1980) and references therein.
- ³⁵See also A. D. Wilson-Gordon, R. Klimovsky-Barid, and H. Friedmann, *Phys. Rev. A* **25**, 1580 (1982).
- ³⁶J. Mlynek, F. Mitschke, E. Köster, and W. Lange in *Proceedings of the Fifth Rochester Conference on Coherence and Quantum Optics*, Rochester, New York, June 1983 (in press).